Linear instabilities in the wakes of cylinders with triangular cross-sections

Z. Y. Ng, T. Vo, W. K. Hussam and G. J. Sheard

Department of Mechanical and Aerospace Engineering
Monash University, Clayton, Victoria 3168, Australia

Abstract

The wakes of flows past bluff bodies are known to undergo several transitions leading to turbulence, each incurring changes to the dynamics of the flow. The initial transition to three-dimensional flow for several cylindrical geometries manifests as coherent structures along the cylinder span and have been the focus of many investigations. This transition and its associated instability modes are investigated numerically for flows past a cylinder with triangular cross-section at various inclinations using Floquet stability analysis. The instabilities are shown to be strongly dependent on the cylinder inclination, producing a dominant synchronous instability mode consistent with the synchronous Mode A and the subharmonic Mode C at various cylinder inclinations. The neutral stability threshold ranges approximately from $100 < Re_h < 140$, where h is the projected frontal height of the cylinder; and the wavelengths of the instabilities ranging approximately between $4h$–$6h$ for the synchronous mode and approximately $2h$ for the subharmonic mode at transition for various cylinder inclinations.

Introduction

The study of flow transitions and its mechanism, while fundamental in nature, is pivotal in developing a deeper understanding of fluid dynamics. For cylindrical bodies, as the Reynolds number (Re) is increased, the initially steady flow becomes unstable to a two-dimensional time-dependent flow through a Hopf bifurcation. The flow then becomes three-dimensional upon further increasing Re, exhibiting finger-like structures from the onset. [1, 15, 17, 18] showed that these secondary flow instabilities for the circular cylinder manifests via an instability termed Mode A which becomes unstable at $Re \approx 190$, and later through an instability named Mode B at $Re = 259$—a review of these wake instabilities and their characteristics can be found in [19].

Further investigations on various bluff-bodies also reveal the existence of a subharmonic instability mode coined Mode C. This mode was observed in the wakes of rings at moderately low aspect-ratios (AR), while the synchronous modes were observed at higher AR's as the geometry tended to a circular cylinder [14]. The instability pathway of the wake of a normally oriented square cylinder demonstrated a similar route to instability as the circular cylinder with the exception of an additional instability branch [11]; [13] showed this instability to grow stronger at intermediate inclination angles, eventually becoming dominant over the synchronous mode branches. Further studies by [3, 12] showed this subharmonic mode to smoothly take over from the quasi-periodic mode when the reflection symmetry about the wake centreline is gradually broken. The synchronous instability modes appear to bifurcate from a base-flow exhibiting symmetries of the Kármán vortex street [2], a lack thereof introduces the Mode C instability with a period-doubling mechanism to recover some sense of periodicity.

We set out to further investigate the dependence of the transition scenario on underlying asymmetries in the dynamic wake, which for this study, was produced from a triangular cylinder
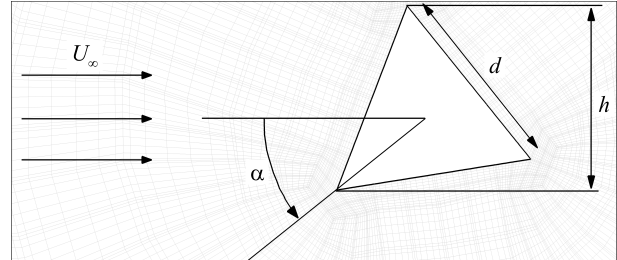

Figure 1: System set-up with the cylinder inclined at an angle α. The background displays the resolution of the mesh used.

at various inclination angles. The only available data on the stability of these flows in literature comes from [9], who experimentally studied the three-dimensional wake transition for a single isosceles triangular cylinder pointing downstream and reported Mode A to become unstable at $Re \approx 164$.

Methodology

For this study, a fluid of velocity U_∞ is incident on a triangular cylinder at an inclination α, producing a wake region whose stability characteristics are sought. A schematic of this system is provided in figure 1. The cylinder inclination was gradually varied between $0° \leq \alpha \leq 60°$, generally at an increment of $6°$, with all other inclinations outside this range being either reflection symmetric about the horizontal centreline, or identical, to the geometries contained within the initial range. Specifically, $\alpha = 0°$ corresponds to the case with the triangle pointing directly upstream, $\alpha = 60°$ describes the triangle pointing directly downstream, and $\alpha = 90°$ corresponds to the cylinder at $\alpha = 30°$ flipped vertically about the horizontal centreline. Lengths in this study are scaled by the height of the cylinder projected on the fluid (h), speeds by the uniform inflow velocity (U_∞), time by h/U_∞, and pressure by ρU_∞^2. The hydrodynamics of this system is thus governed by α and Re, where $Re = U_\infty h/\nu$.

Numerical Formulation

The flows considered in this study are governed by the incompressible Navier–Stokes equations

$$\nabla \cdot \boldsymbol{u} = 0, \tag{1a}$$

$$\frac{\partial \boldsymbol{u}}{\partial t} + (\boldsymbol{u} \cdot \nabla)\, \boldsymbol{u} = -\nabla p + \frac{1}{Re}\, \nabla^2\, \boldsymbol{u}. \tag{1b}$$

If a three-dimensional perturbation field ($\{\boldsymbol{u}', p'\}$) is imposed on a time-periodic two-dimensional base-flow homogeneous in the cylinder spanwise direction ($\{\bar{\boldsymbol{u}}, \bar{p}\}$), the linearised model for the evolution of the perturbation field can be derived as

$$\nabla \cdot \boldsymbol{u}' = 0, \tag{2a}$$

$$\frac{\partial \boldsymbol{u}'}{\partial t} + (\boldsymbol{u}' \cdot \nabla)\, \bar{\boldsymbol{u}} + (\bar{\boldsymbol{u}} \cdot \nabla)\, \boldsymbol{u}' = -\nabla p' + \frac{1}{Re}\, \nabla^2\, \boldsymbol{u}'. \tag{2b}$$

Representing the perturbation field $\{\boldsymbol{u}', p'\}$ with a Fourier expansion following [1], perturbation wavenumbers decouple

from each other in the linearised model, permitting the stability analysis at each Re and α to be performed as a function of the wavenumber (m) alone. The wavenumber is related to the instability wavelength (λ) through $\lambda = 2\pi/m$.

A nodal spectral-element method is used for spatial discretisation [6] in conjunction with a third-order time-integration scheme based on backwards differentiation [4, 5] to evolve the two-dimensional form of the incompressible Navier–Stokes equations (equation 1) to a saturated time-periodic state. Floquet stability analysis is then performed by evolving a three-dimensional perturbation field on the time-periodic base-flow using the linearised model (equation 2) [1], and the complex eigenmodes of the periodic system evaluated using the ARPACK package [7]. The complex eigenvalues correspond to the Floquet multipliers of the system (μ), which are related to the instability growth rates (σ) through $|\mu| = \exp(\sigma T)$, where T is the period of the two-dimensional base-flow. The flow is thus linearly unstable when the growth rate $\sigma > 0$ ($|\mu| > 1$), and its nature is one of either synchronous if the system's eigenvalue is positive real, subharmonic if negative real, or quasi-periodic if an imaginary component is present. The critical Re for flow transition is estimated as the Re where the instability growth rate $\sigma = 0$. The two-dimensional flow solver and Floquet analysis routine have been implemented and validated in various wake-flow studies [3, 13]. Validation of the meshes and computational domain used in this study can be found in [10].

Boundary Conditions

To simulate an unbounded flow through the computational domain, a streamwise velocity of U_∞ was imposed at the inlet while stress-free, impermeable boundaries were assigned at the transverse walls. The outlet was treated with a standard pressure outflow boundary condition and a zero outward-normal gradient of velocity, while the body was given a no-slip condition. A high-order Neumann boundary condition was imposed on the outward-normal gradient of pressure at all boundaries with a Dirichlet condition on the velocity to maintain the overall third-order accuracy of the scheme [5].

Results

The structure and characteristics of the two-dimensional base-flows for this system at various α and Re are discussed in [10]. The Floquet analysis requires the base-flow to be time-periodic which limits the range of Re where this analysis can be performed—higher Re flows quickly develop a spatial instability where a secondary vortex street forms and introduces incommensurate frequencies into the wake. Within the range of available Re, the two-dimensional vortex street resembles the familiar Kármán vortex street with counter-rotating vortices shed from the body in succession which then rapidly decays as it advects downstream.

Gradually increasing the cylinder inclination angle invokes gradual changes to growth rate profile across the range of wavenumbers investigated. At low angles of $\alpha < 24°$, a single dominant peak is observed at wavenumbers similar to the Mode A instability behind a circular cylinder, and is also synchronous to the base-flow. Within $18° < \alpha < 36°$, a subharmonic mode peak appears, although the synchronous mode branch remains dominant (figure 2). This subharmonic mode becomes unstable beyond $\alpha \approx 34°$, with other inclinations within this range showing the growth rate reaching a maximum negative value before decreasing at higher Re. The subharmonic instability mode becomes the first occurring mode at $\alpha \approx 34.6°$. From $36° < \alpha < 54°$, the growth rate profile shows only a dominant subharmonic peak at wavenumbers similar to Mode C behind
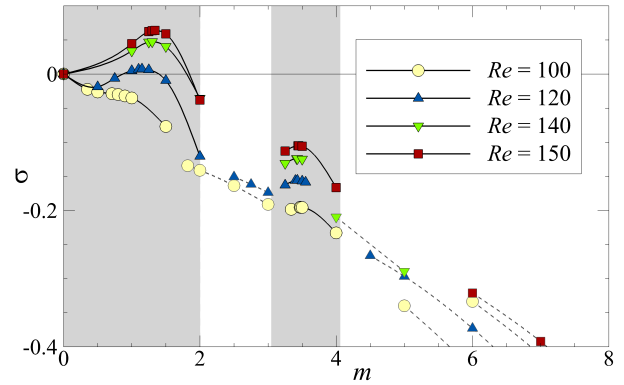

Figure 2: An atypical growth rate vs wavenumber curve across various Re, here for $\alpha = 24°$. Grey shaded regions denote wavenumber domains where the instability modes typically exhibited a local maximum, while non-shaded regions typically contain quasi-periodic mode branches. Low/high α cases usually show only a single peak at either shaded regions, with two-local-maxima profiles occurring over approximately $18° \lesssim \alpha \lesssim 36°$ within the range of Re investigated.

ring cross-sections [14]. The synchronous mode branch re-appears at $\alpha \approx 54°$, and resumes as the first occurring instability at $\alpha \approx 55.4°$. For the range of Re investigated, instabilities consistent with the synchronous Mode B branch and quasi-periodic modes were not observed as they usually manifest at much higher Re exceeding the upper bound limitation in this study.
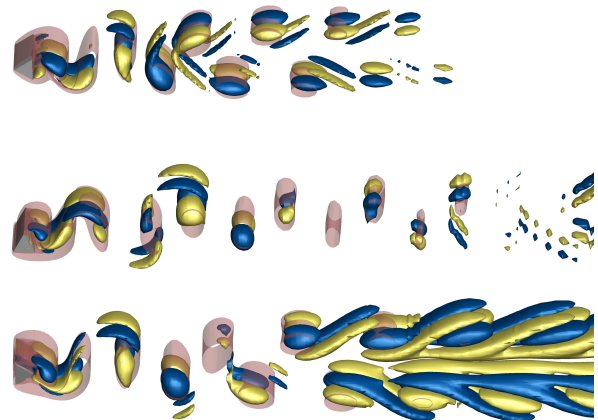

Figure 3: (*top to bottom*) Visualisation of the leading eigenmode superimposed on the two-dimensional base-flow for the cylinder inclined at $\alpha = 0°$, $30°$, and $60°$. Blue/yellow isosurfaces represent positive/negative streamwise vorticity in the leading eigenmode at arbitrary levels to visualise the instability, and translucent red isosurfaces outline the two-dimensional vortex loops.

The structure of the synchronous instability mode is visualised for the cylinder inclined at $\alpha = 0°$, $30°$, and $60°$ (figure 3). Consider the near wake region of the perturbation fields; the instability structure appears to be strongest in the core of the two-dimensional vortices, and also qualitatively possesses the 'half-period-flip' symmetry much like the Mode A instability [8]—in this case, the two 'half-periods' that make a full shedding period are not of the same length due to the asymmetry in the wake induced by the cylinder's inclination. Due to this similar-

ity, this synchronous instability will also be referred to as Mode A [13, 14]. The structure of the subharmonic mode, shown in figure 4, instead resembles the Mode C instability. The structure is periodic to two shedding cycles of the base flow, and will hereafter be referred to as Mode C [13, 14].
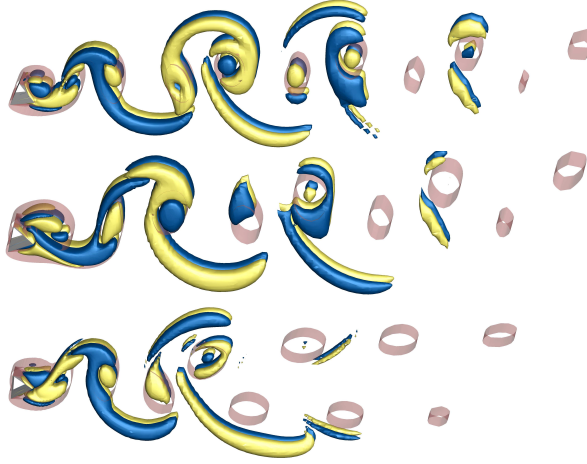

Figure 4: (*top to bottom*) Visualisation of the instability mode for flows past the cylinder inclined at $\alpha = 36°$, $45°$, and $54°$. Contour levels and colors are as per figure 3.

Interpolating the instability growth rates across Re to zero growth rate at each α yields the transition Re at various cylinder inclinations. The neutral stability curve for this system is shown in figure 5. As described previously, the Mode A instability manifests over all inclinations α except within $34° < \alpha < 56°$ where Mode C takes over as the first occurring, and for most cases also the only observable, instability. The Mode A to Mode C switching is predicted to occur at $\alpha \approx 34.6°$ and the subsequent Mode C to Mode A switching at $\alpha \approx 55.4°$. For the transition Re for Mode A (Re_A), a small kink is observed in the curve from $\alpha \approx 28°$, but is smoothed out upon re-scaling Re by the cylinder side length d—the Re_A curve remains deflected at a different gradient for $\alpha \geq 30°$. This could be related to the fact that $\alpha = 30°$ separate two cases where the cylinder appears topologically different to the flow—one case presents a single cylinder face in the downstream direction for the recirculation region to form over while the other presents two—the two-dimensional wakes and dynamics of both scenarios demonstrate several differences [10, 16]. The two-dimensional wake appears to be most unstable overall at low cylinder inclinations where the triangle points upstream, exhibiting the Mode A instability. The Mode A branch at higher α where the triangle points downstream appears almost as stable as the initial Mode A branch close to the Mode C switch. Results for the wake behind an isosceles triangular cylinder [9] oriented similarly to the present cylinder at $\alpha = 60°$ shows an even higher transition threshold at $Re_A = 164$ without any observation of the Mode B instability. This highlights the effects of the afterbody geometry on flow stability. The Mode C instead appears to be most unstable at $\alpha \approx 45°$. It is interesting to note that the square cylinder wake becomes unstable to Mode C at a much lower inclination angle of $10.5°$ [12, 13], and appears most unstable at an inclination of approximately $24°$ where the square cross-section geometry would be approximately most asymmetric about the horizontal centreline. Conversely, the triangular cylinder at $\alpha \approx 45°$ is not as geometrically asymmetrical as it is at $\alpha \approx 30°$, but yet shows the Mode C to be most unstable for the former while the latter inclination remains unstable only to Mode A. Using the lift coefficient as a measure of asymmetries in the wake and
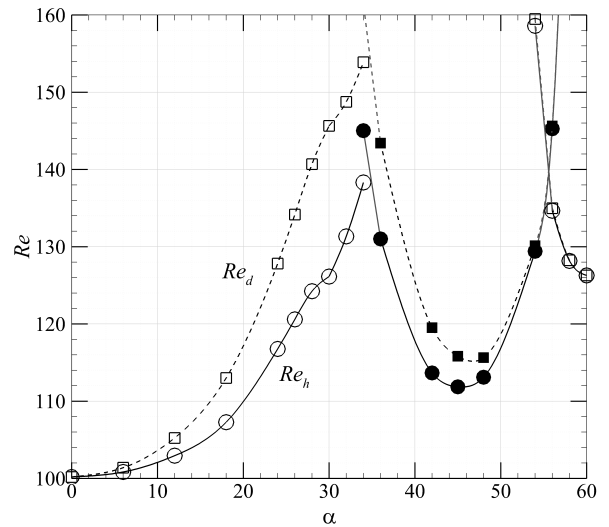

Figure 5: Neutral stability curves above which the linear instability manifests. Solid connecting lines through circular markers weave through transition Re scaled by h while dashed lines through square markers connect the transition Re scaled by d. Hollow symbols mark Mode A transitions, while filled symbols mark Mode C.

flow-field about the body revealed no correlation with the stability of Mode C—[10] reported the lift coefficient to be highest for $\alpha \approx 30°$, with no discerning pattern observed at $\alpha \approx 45°$.

The wavelengths of the two occurring instabilities for the flow in critical state at various cylinder inclinations are shown in figure 6. The three discontinuous branches correspond directly to the two Mode A branches and the Mode C branch depicted in figure 5. For the low-α Mode A branch, the instability wavelength (λ_A) appears strongly dependent on the cylinder inclination starting at $\lambda_A \approx 5.8h$ at an inclination of $0°$ and increasing to $\lambda_A \approx 6.1h$ at $\alpha \approx 18°$. λ_A was observed to decrease smoothly from inclinations $24°$ to $30°$, and again from $30°$ to approximately $35°$ where Mode C is expected to become dominant, the latter exhibiting a more rapid decrease in wavelength which is perhaps related to the change in gradient in the corresponding Re_A curve at these inclinations (figure 5). The Mode A branch at higher cylinder inclinations on the other hand possesses a more consistent wavelength, with λ_A decreasing from $4.3h$ at $\alpha = 56°$ to $4.2h$ at $\alpha = 60°$. Results for λ_A for the two different Mode A branches appear significantly different, with the smallest λ_A of the low-α Mode A branch being $\approx 4.7h$, while the largest λ_A for the higher α Mode A branch being $\approx 4.3h$. Comparing these values to those arising from other bluff-body wakes show λ_A of the low-α Mode A branch (re-scaled by the cylinder side length d as shown in figure 6) to be similar to that from the square cylinder wake ($\lambda_A \approx 4.2$ to 5.7 times the square cylinder side length [13]), and λ_A of the higher α Mode A branch to be similar to that of the circular cylinder's Mode A ($\lambda_A \approx 3.96$ times the cylinder diameter [1]). The instability wavelength of the subharmonic Mode C (λ_C) instead appears consistent at $\lambda_C \approx 1.6h$–$1.8h$, in agreement with values quoted from previous studies [13, 14].

Conclusions

The stability of the wakes produced by a triangular cylinder at various inclination angles (α) is elucidated. Transition from two- to three-dimensional flow is predicted to manifest through either a synchronous instability mode consistent with Mode A
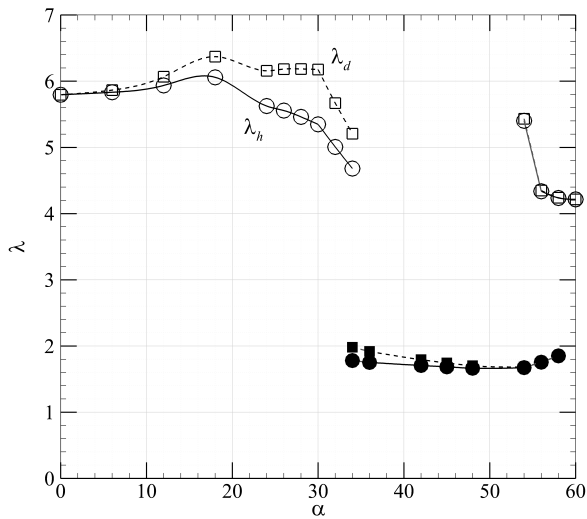
Figure 6: Predicted instability wavelength at transition. Markers and lines used are as defined in figure 5.

or the subharmonic Mode C at various ranges of α. For inclinations up to $\alpha \approx 34°$, the wake becomes unstable through an instability consistent with Mode A with little or no indication of Mode C becoming unstable; the transition *Re* for this instability mode increasing with α. This instability mode is lost for $\alpha \gtrsim 36°$ but becomes observable again at higher inclinations of $\alpha \gtrsim 56°$ as the geometry and wake approximately recovers a streamwise symmetry. Both aforementioned instabilities possess initial wavelengths of approximately $4.7h$–$6.1h$ at low α and later approximately $4.2h$–$4.3h$ when the instability mode becomes the first-occurring again.

At intermediate inclination angles from approximately $\alpha = 36°$ to $\alpha = 54°$, the subharmonic Mode C was predominantly the only instability observed over the range of wavenumbers, lacking the synchronous mode branch almost entirely. The instability wavelength decreases from approximately $1.8h$–$1.6h$ with increasing α at its onset. It is interesting to note that this instability mode appears to be most unstable at an angle $\alpha \approx 45°$, which contrasts to previous studies showing the Mode C to be stronger in wakes with stronger asymmetries induced by the geometry—the wake at $\alpha \approx 30°$ possesses the largest lift coefficient (associative with least symmetry in the flow field about the body) but still shows the synchronous instability mode to develop even past this inclination. Further direction for this study could attempt to determine the metrics of any wake asymmetries present, and features of the flow which give rise to, and amplifies, the Mode C instability.

Acknowledgements

References

[1] Barkley, D. and Henderson, R. D., Three-dimensional Floquet stability analysis of the wake of a circular cylinder, *J. Fluid Mech.*, **322**, 1996, 215–241.

[2] Blackburn, H. M., Marques, F. and Lopez, J. M., Symmetry breaking of two-dimensional time-periodic wakes, *J. Fluid Mech.*, **522**, 2005, 395–411.

[3] Blackburn, H. M. and Sheard, G. J., On quasiperiodic and subharmonic Floquet wake instabilities, *Phys. Fluids*, **22**, 2010, 031701.

[4] Blackburn, H. M. and Sherwin, S. J., Formulation of a Galerkin spectral element-Fourier method for three-dimensional incompressible flows in cylindrical geometries, *J. Comput. Phys.*, **197**, 2004, 759–778.

[5] Karniadakis, G. E., Israeli, M. and Orszag, S. A., High-order splitting methods for the incompressible Navier–Stokes equations, *J. Comput. Phys.*, **97**, 1991, 414–443.

[6] Karniadakis, G. E. and Triantafyllou, G. S., Three-dimensional dynamics and transition to turbulence in the wake of bluff objects, *J. Fluid Mech.*, **238**, 1992, 1–30.

[7] Lehoucq, R., Sorensen, D. and Yang, C., *ARPACK Users' Guide*, Society for Industrial and Applied Mathematics, 1998.

[8] Leweke, T. and Williamson, C. H. K., Three-dimensional instabilities in wake transition, **17**, 1998, 571–586.

[9] Luo, S. C. and Eng, G. R. C., Discontinuities in the S-Re relations of trapezoidal and triangular cylinders, 2010, volume 7522, 75221B–75221B–10, 75221B–75221B–10.

[10] Ng, Z. Y., Vo, T., Hussam, W. K. and Sheard, G. J., Two-dimensional wake dynamics behind cylinders with triangular cross-section under incidence angle variation, *J. Fluids Struct.*, **63**, 2016, 302–324.

[11] Robichaux, J., Balachandar, S. and Vanka, S. P., Three-dimensional Floquet instability of the wake of square cylinder, *Phys. Fluids*, **11**, 1999, 560–578.

[12] Sheard, G. J., Wake stability features behind a square cylinder: Focus on small incidence angles, *J. Fluids Struct.*, **27**, 2011, 734–742.

[13] Sheard, G. J., Fitzgerald, M. J. and Ryan, K., Cylinders with square cross-section: wake instabilities with incidence angle variation, *J. Fluid Mech.*, **630**, 2009, 43–69.

[14] Sheard, G. J., Thompson, M. C. and Hourigan, K., From spheres to circular cylinders: the stability and flow structures of bluff ring wakes, *J. Fluid Mech.*, **492**, 2003, 147–180.

[15] Thompson, M., Hourigan, K. and Sheridan, J., Three-dimensional instabilities in the wake of a circular cylinder, *Exptl. Thermal Fl. Sci.*, **12**, 1996, 190–196.

[16] Tu, J., Zhou, D., Bao, Y., Han, Z. and Li, R., Flow characteristics and flow-induced forces of a stationary and rotating triangular cylinder with different incidence angles at low Reynolds numbers, *J. Fluids Struct.*, **45**, 2014, 107–123.

[17] Williamson, C. H. K., The existence of two stages in the transition to three-dimensionality of a cylinder wake, *Phys. Fluids*, **31**, 1988, 3165–3168.

[18] Williamson, C. H. K., Three-dimensional wake transition, *J. Fluid Mech.*, **328**, 1996, 345–407.

[19] Williamson, C. H. K., Vortex dynamics in the cylinder wake, *Annu. Rev. Fluid Mech.*, **28**, 1996, 477–539.